Direct Synthesis of Nickel(II) Tetraphenylporphyrin and Its Interaction with a Au(111) Surface: A Comprehensive Study

Min Chen,[†] Xuefei Feng,[†] Liang Zhang,[†] Huanxin Ju,[†] Qian Xu,[†] Junfa Zhu,*[,†] J. Michael Gottfried,*[,‡] Kurash Ibrahim,[§] Haijie Qian,[§] and Jiaou Wang[§]

National Synchrotron Radiation Laboratory, University of Science and Technology of China, Hefei 230029, People's Republic of China, Universität Erlangen-Nürnberg, Lehrstuhl für Physikalische Chemie II, Egerlandstr. 3, 91058 Erlangen, Germany, and Laboratory of Synchrotron Radiation, Institute of High Energy Physics, Chinese Academy of Sciences, Beijing 100049, People's Republic of China

Received: March 5, 2010; Revised Manuscript Received: April 19, 2010

Tetraphenylporphyrin (2HTPP) molecules were vapor-deposited onto a gold(111) surface to serve as reactive ligands for the direct synthesis of nickel(II) tetraphenylporphyrin (NiTPP) under ultrahigh vacuum (UHV) conditions. The surface-confined coordination reaction between a 2HTPP monolayer and coadsorbed Ni as well as the structure of 2HTPP multilayer films on Au(111) was characterized in detail using synchrotron radiation photoelectron spectroscopy (SRPES), X-ray photoelectron spectroscopy (XPS), and near-edge X-ray absorption fine structure spectroscopy (NEXAFS). It is shown that the vapor-deposited 2HTPP multilayer on Au(111) has a high degree of ordering with a preferential orientation of the molecular plane relative to the substrate. Monolayers of 2HTPP on Au(111) were obtained by annealing the 2HTPP multilayers to 520 K and were found to be thermally stable up to at least 580 K. NiTPP can be synthesized directly on the Au(111) surface through reaction of the 2HTPP monolayer with postadsorbed Ni atoms. The same reaction occurs if Ni is deposited prior to the deposition of 2HTPP. It is proposed that the complete and uniform metalation of the porphyrin layer is possible because the Ni atoms can diffuse easily on the porphyrin-covered surface. Ni 2p XP spectra of NiTPP monolayers indicate that the electronic interaction between the coordinated Ni ion and the Au substrate is weak.

1. Introduction

Porphyrins and other tetrapyrrolic macrocycles are ubiquitous in nature and play an important role in different fields ranging from medicine to material science. Their metal complexes, the metalloporphyrins, are the active centers of many enzymes.[1] Together with other functional planar metal complexes, metalloporphyrins are of considerable technological importance, for instance as convenient building blocks for the design of supramolecular architectures.[2,3] Since porphyrins have strong absorption bands in the ranges 400−430 and 550−600 nm,[4] they can be potential candidates for the construction of functional photonic devices[2] and act as photosensitizers in light-harvesting systems such as dye-sensitized solar cells.[5] Notably, the physicochemical properties of the porphyrin materials can easily be tuned, e.g., by adding specific substituent groups to the porphyrin macrocycle. These new materials can be exploited for the development of novel biomimetic and other model systems for investigating biological functions.

Thin porphyrin films have received significant fundamental research interest with respect to the fabrication of chemical sensors,[6] photovoltaic cells,[7] and organic light-emitting diodes.[8] In recent years, Langmuir−Blodgett films,[9] self-assembled monolayers from solution,[10] and self-organized structures[11] of porphyrins have been studied by a wide variety of techniques, e.g., near-edge X-ray absorption fine structure (NEXAFS),[10] X-ray photoelectron spectroscopy (XPS),[12] and scanning tunneling microscopy (STM).[11,13] Compared to the thin films made under ambient conditions, vapor deposition of porphyrins onto inert metal surfaces under ultrahigh vacuum (UHV) conditions leads to especially clean and well-defined thin films. Metalloporphyrin monolayers have also been used recently for fundamental studies in the emerging field of surface coordination chemistry.[14] The related studies focused on surface reactions such as direct porphyrin metalation[15−21] and coordination of additional ligands[17,22] as well as on the character of the surface coordinative bond.[23−26] The direct metalation of porphyrin layers with metal atoms in UHV is especially interesting for the in situ synthesis of reactive complexes such as Fe(II) porphyrins, which are very oxygen-sensitive and therefore difficult to handle outside the vacuum.[18−21] The metalation is a redox reaction resulting in the oxidation of the metal and a reduction of the porphyrin ligand; it was studied for various porphyrin ligands with different substituents and for different metals, namely Co,[15,16] Fe,[18−21] Zn,[17,27] and Ce.[28] The substrate used in these studies was Ag(111), in one case also Cu(100).[29]

Further investigations focused on the molecular arrangement[23,30−34] as well as on the electronic interaction between the coordinated metal ion and the substrate.[23−26] X-ray and UV photoelectron spectroscopy (XPS/UPS)[19,24−26] and scanning tunneling microscopy/spectroscopy (STM/STS)[23] revealed that for example the coordinated Co and Fe ions in the porphyrin monolayer interact strongly with an Ag(111) substrate, but less so with Au(111).[26] In contrast, Zn ions appear to be much more inert, which has been attributed to the relatively low energy of the Zn 3d orbitals.[14,27] Since the 3d orbital energies decrease in the order Fe > Co > Ni > Cu > Zn, the Ni ion is an interesting

* To whom correspondence should be addressed. E-mail: jfzhu@ustc.edu.cn (J.Z.), michael.gottfried@chemie.uni-erlangen.de (J.M.G.).
[†] University of Science and Technology of China.
[‡] Universität Erlangen-Nürnberg.
[§] Chinese Academy of Sciences.

10.1021/jp102031m
Published on Web 05/13/2010

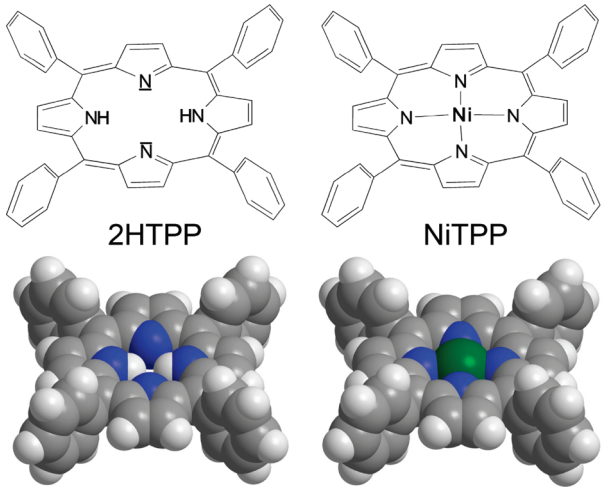

Figure 1. Structural formula and space-filling model of 2HTPP (left) and NiTPP (right).

transition case between the strongly (Fe, Co) and weakly (Zn) interacting ions; its study can hence provide new insight into the surface coordinative bond in general.

Ni is also an especially interesting case with respect to the direct metalation reaction because previous density functional theory (DFT) studies of the reaction mechanism predict increasing activation barriers in the order Fe < Co < Ni < Cu < Zn. Fe and Co should react at room temperature, whereas Cu and Zn require elevated temperatures of up to 500 K for rapid reaction. These predictions have been experimentally verified for Fe, Co, and Zn, and excellent agreement between experimental and theoretical activation energies was found for Zn.[15] In the case of Ni, the broad range of calculated activation barriers (between 45 and 121 kJ/mol, depending on the functional used)[15] makes it questionable whether room-temperature metalation is possible or not. The present study will show that metalation indeed occurs at room temperature, indicating that the activation energy is well below 121 kJ/mol.

The above considerations are motivation to study the formation of nickel(II)−tetraphenylporphyrin (NiTPP, see Figure 1) by reaction of adsorbed tetraphenylporphyrin (2HTPP) on Au(111) with coadsorbed Ni atoms. We will also show that 2HTPP is able to react with predeposited Ni on Au(111), a reaction that has previously only been observed for Fe and Zn on Ag(111).[19,27] In addition, the interaction of NiTPP with the Au(111) substrate surface will be investigated in detail with XPS. In related previous work, mono- and bilayers of the unsubstituted Ni(II) porphine on Ag(111) were studied by STM and show the formation of ordered hexagonal structures.[35] NiTPP multilayer films on polycrystalline Au have been studied by UPS.[31] Because of the thickness of the layer (4 nm), no information on the electronic structure of the NiTPP/Au interface was obtained. In this work, we will study NiTPP on Au(111) by XPS to obtain information about the interaction between porphyrin-coordinated Ni(II) ions and a Au(111) surface.

The molecular orientation and arrangement of porphyrin films on well-ordered metal substrates is another important aspect, which has in the past mainly been studied on molecular monolayers by STM[19,23,31−34,36−38] and NEXAFS.[36,39−44] However, to our knowledge, much less attention has been paid to the structures of multilayer porphyrins on metal substrates so far.[39,45,46] The multilayer structure is important for the usage of porphyrins and other tetrapyrroles such as phthalocyanines in organic electronic devices,[47−49] since the molecular arrangement and orientation are crucial for parameters such as charge carrier mobilities and thus for the efficiency of the devices.[50] In the present work, we will employ NEXAFS to investigate the ordering and conformation of 2HTPP multilayers on Au(111). (STM was not used here, since studies of molecular multilayers are very challenging with this technique.)

This paper is organized as follows: After a description of the experimental setup and procedure, NEXAFS measurements of a vapor-deposited multilayer 2HTPP film on Au(111) are presented. Next, the temperature-dependent evolution of multilayers of 2HTPP and NiTPP to monolayers, monitored by temperature-dependent XPS, are shown. After that, we will describe the metalation of a 2HTPP monolayer with incremental amounts of Ni atoms, as was investigated in situ by synchrotron-based photoemission spectroscopy. Finally, XP spectra for the reaction of 2HTPP molecules with predeposited Ni atoms are discussed.

2. Experimental Section

The experiments were performed in two separate ultrahigh vacuum (UHV) systems. For most of the XPS measurements, a VG MARK II spectrometer was employed. This spectrometer comprises two UHV chambers separated by a gate valve. The analysis chamber has a base pressure below 2×10^{-10} Torr and is equipped with a hemispherical electron analyzer, a twin-anode X-ray source for XPS, and an electron gun for AES. The preparation chamber with a base pressure of 3×10^{-10} Torr comprises a set of four-grid LEED optics (SPECS ErLEED), a cold cathode ion gun for sample cleaning, a mass spectrometer (Pfeiffer QMG 220), and several evaporators. The overall energy resolution for XPS was 0.9 eV. During XPS measurements, the photoelectrons were detected at an angle of 70° with respect to the surface normal for increased surface sensitivity. All reported binding energies were referenced to the Fermi edge of the clean Au surface.

NEXAFS and synchrotron-based core level spectra were acquired in the Photoelectron Spectroscopy Endstation at the 4B9B beamline of the Beijing Synchrotron Radiation Facility. This endstation consists of an analysis chamber and a sample preparation chamber, allowing in situ film preparation, and contains devices for direct sample transfer from the preparation chamber to the analysis chamber for NEXAFS and photoemission experiments. The analysis chamber has a base pressure of 2×10^{-10} Torr and is equipped with a VSW hemispherical electron analyzer and LEED optics. The sample preparation chamber has a base pressure of 5×10^{-10} Torr and is equipped with several evaporators. The 4B9B beamline offers soft X-rays with energies ranging from 60 to 1100 eV, a typical photon flux of 10^{10} photons/s at the sample position, and a resolving power ($E/\Delta E$) better than 1000. NEXAFS measurements at the K-shell absorption edges of C and N were carried out in total electron yield (TEY) mode by monitoring the drain currents from the sample. Linearly polarized soft X-rays with a polarization factor, P, of ≈75% were used. NEXAFS raw spectra were first normalized by the incident beam intensity, which was measured concomitantly using the photoelectron yield of a gold grid located upstream from the analysis chamber, and then divided by the signal of a reference absorption spectrum taken under the same experimental conditions on a clean Au(111) surface.[51] After that, in order to normalize all the signals to the number of sampled C or N atoms, a pre-edge background was subtracted from the divided spectra. Finally, the spectra were normalized to the absorption edge jump, which was arbitrarily set to unity.[51,52] The N 1s and Ni 2p core-level spectra were

taken with photon energies of 500 and 970 eV, respectively, to optimize surface sensitivity. To eliminate possible peak shifts caused by fluctuations of the photon energy, Au 4f photoelectron spectra were recorded before each measurement using a polycrystalline Au foil. Position (84.00 eV for Au $4f_{7/2}$) and intensity of this signal were used to calibrate the photon energy and intensity, respectively.

2HTPP and NiTPP (Figure 1) were used as supplied (purity >98%, Porphyrin Systems GbR). It has been shown previously that porphyrins can be thermally deposited onto gold without changes in chemical composition or oxidation state.[24,26,33] We adopt this method to prepare thin films of 2HTPP and NiTPP on Au(111). 2HTPP was evaporated from a Knudsen cell evaporator with an alumina crucible and NiTPP from a home-built Ta metal box evaporator. Both materials were thoroughly degassed *in vacuo* for 20 h at 450 K prior to evaporation. Ni was evaporated from a wire filament with purity of >99.999%. The deposition rate was 0.04 Å/s, as estimated based on the attenuation of the Au 4f signal when Ni was evaporated directly onto Au(111). The substrate was a discoidal Au single crystal with a diameter of 10 mm (purity >99.999%, thickness 2 mm, purchased from MaTeck GmbH). Its polished (111) surface was aligned to <0.4° with respect to the nominal orientation. The clean surface was obtained by repeated cycles of Ar^+ ion sputtering followed by annealing at 700 K until no carbon and oxygen were detectable by XPS, and a sharp (1 × 1) LEED pattern was achieved. In order to precisely measure the sample temperature, a K-type thermocouple was spot-welded directly onto the edge of the Au crystal. The sample was mounted to a sample holder which allows for cooling and heating in the temperature range of 100−1200 K.

In this paper, "monolayer" is used to characterize a saturated layer of molecules, i.e., the maximum number of molecules in direct contact to the substrate surface at 300 K. The coverage θ is defined as the number of adsorbed molecules divided by the number of the substrate surface atoms. It has been found previously that monolayers of 2HTPP and metallotetraphenylporphyrins on a Ag(111) surface correspond to $\theta = 0.037$, as determined by LEED and STM.[18−20,24,31] Since Au and Ag have the same crystal structure and almost identical unit cell dimensions ($a = 4.085$ Å for Ag and $a = 4.078$ Å for Au),[53] we assume that monolayer coverage for 2HTPP and NiTPP on Au(111) is very close to 0.037.

3. Results and Discussion

3.1. Ordering and Conformation of 2HTPP on Au(111). Our first aim is to confirm that the 2HTPP molecules (Figure 1) stay intact upon vapor deposition and to explore their orientation in multilayer films on Au(111) at 300 K. Polarization-dependent X-ray absorption spectroscopy is an ideal tool to investigate the molecular ordering of thin organic films. In principle, the resonance in electronic transitions from a core level initial state of a specific atomic species to unoccupied π^* or σ^* molecular orbitals is strong when the electric field vector E of the incident linearly polarized synchrotron light has a large projection along the direction of the π^* or σ^* orbital, and it vanishes when E is perpendicular to the orbitals.[51] Therefore, the orientation of the transition dipole moment (TDM) of the probed molecules relative to the polarization of the incoming light determines the intensity of the NEXAFS resonances and thus provides information on the ordering and average orientation of adsorbed molecules.

Figures 2 and 3 show the C and N K-edge NEXAFS spectra at different X-ray incident angles for a multilayer 2HTPP on

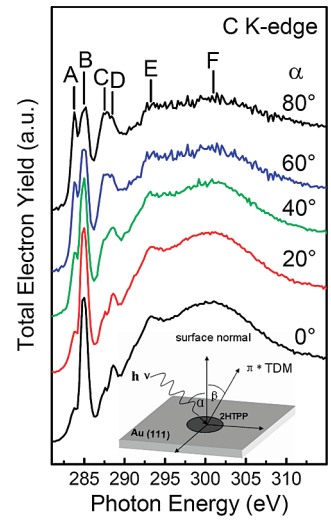

Figure 2. C K-edge NEXAFS spectra of a multilayer 2HTPP film (~7 monolayers) on Au(111) at different X-ray incident angles. The inset shows the geometry of the experiment.

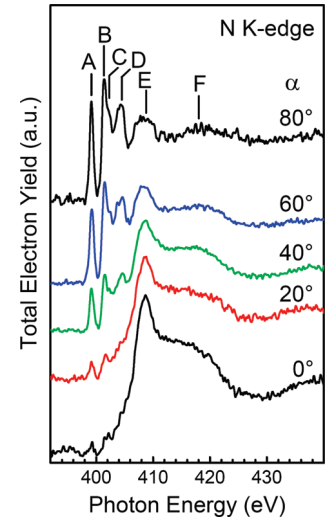

Figure 3. N K-edge NEXAFS spectra of a multilayer 2HTPP film (~7 monolayers) on Au(111) at different X-ray incident angles (see inset of Figure 1 for details of the experimental geometry).

Au(111) at 300 K, respectively. The chemical structure of the molecule is depicted in Figure 1, and the experimental geometry is shown in the inset of Figure 2. Angle-dependent NEXAFS data were obtained here by rotating the sample. Both the C and N K-edge NEXAFS spectra were recorded at X-ray incidence angles of 0°, 20°, 40°, 60°, and 80° relative to the sample surface normal. When varying the light incident angle, the intensity of each peak changes dramatically, indicating the formation of a well-ordered 2HTPP multilayer with preferential molecular orientation, which will be discussed in more detail below.

The C K-edge NEXAFS spectra in Figure 2 show six resonance features, labeled A−F, in the π^* and σ^* regions. These features are centered at 283.8, 284.9, 287.6, 288.6, 293, and 301 eV, respectively. A and C show the same angular dependence; i.e., their intensities increase with the incident angle. Following the previous interpretations of C K-edge NEXAFS spectra of ZnTPP[45] and porphine multilayers[39] on Si(111), as well as spectra of ZnTPP on Ag films,[46] these peaks are attributed to C 1s → π^* resonances at the carbon atoms in the porphyrin ring. In detail, peak A reflects the electronic transitions from the C 1s level to the lowest unoccupied molecular orbital (LUMO), which is a π_1^* orbital mainly localized at the porphine

macrocycle, while peak C is a transition of the C 1s electrons into the second antibonding π_2* orbital of the porphyrin ring. In contrast to peaks A and C, peak B decreases in intensity as the incident angle α increases, indicating that this feature must be related to C 1s $\rightarrow \pi_1$* resonances localized on the phenyl groups that tilt out of the porphyrin plane.[41,54] This assignment of peaks A and B is especially strongly supported by a previous study, in which the NEXAFS spectrum of ZnTPP was compared with the spectra of zinc octaethylporphyrin and benzene.[45] The small resonance at 288.6 eV (peak D) is associated with a transition of the C 1s electrons into Rydberg states (R*(C−H)) below the ionization edge,[10,55,56] in addition to the contribution from π_2* resonance in the phenyl groups.[10,57] The broad features E and F are σ* resonances; that is, they originate from the excitation of C 1s electrons into the molecular σ* orbitals. These transitions occur at higher photon energies and show an opposite angle-dependent intensity variation compared to the π* resonances of the porphine unit.

The N K-edge NEXAFS spectra shown in Figure 3 were taken under the same conditions as the C K-edge spectra. Five resonance peaks labeled A−E are found at 399.2, 401.4, 402.3, 404.5, and 408.7 eV, respectively, and an additional broader feature (F) appears around 418 eV. As shown in the molecular structure in Figure 1, the 2HTPP molecule contains two nonequivalent nitrogen species, pyrrolic (−NH−) and iminic (=N−) nitrogen, which give rise to two well-resolved peaks in the N 1s XPS signal (see also Figures 7 and 9).[15,16,19,27,58] The resonance peaks A−D correspond to the excitations from the N 1s level to antibonding π* orbitals, while peaks E and F are related to N 1s $\rightarrow \sigma$* excitations.[39,42,46] In detail, peak A can be assigned to the electronic transition from N 1s orbitals at the iminic nitrogens to unoccupied antibonding π_1* orbitals, whereas the peak B is ascribed to the N 1s $\rightarrow \pi_1$* transition at the pyrrolic nitrogens.[39,42] According to the theoretical simulation of the N K-edge spectrum of porphyrin by Narioka et al.[46] and experimental work for porphine by Polzonetti et al.,[39] the resonance peaks C and D are assigned to N 1s $\rightarrow \pi_2$* transitions into the second antibonding π* orbital at the =N− and −NH− nitrogen atoms, respectively. The feature E and F are attributed to σ* (N−C) and σ* (C−C) resonances, respectively.[39,59]

In order to obtain the ensemble-averaged molecular orientation of the thin films, we perform a quantitative analysis of the angular dependence of the NEXAFS resonance intensities based on the procedure by Stöhr.[51] Since the N atoms only belong to the 2HTPP macrocycle and their p_z orbitals are perpendicular to the macrocycle plane, the N K-edge NEXAFS spectra are more useful to obtain the molecular orientation. For this analysis, we choose the most intense feature around 399 eV, peak A, of the N 1s NEXAFS spectra. According to Stöhr,[51] for 3-fold or higher substrate symmetry, the intensity of the π* resonances, I, has a relation with the X-ray incidence angle α and the polar angle β, which is defined as the angle between the corresponding TDM (transition dipole moment, normal to the porphyrin plane) and the surface normal, as follows:

$$I(\alpha,\beta) = A\left\{\frac{1}{3}P\left[1 + \frac{1}{2}(3\sin^2\alpha - 1)(3\cos^2\beta - 1)\right] + \frac{1}{2}(1 - P)\sin^2\beta\right\} \quad (1)$$

The meaning of the angle α is visualized in the inset of Figure 2, A is a proportionality constant, and P is the X-ray polarization factor. By fitting the integrated intensities of the π* resonances as a function of the X-ray incident angle to the equation above,

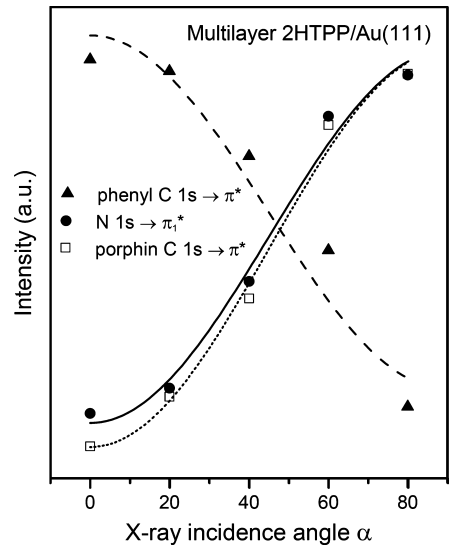

Figure 4. Integrated π* peak intensities as a function of the X-ray incidence angle α, and the corresponding theoretical fits using eq 1, assuming a degree of polarization of $P = 0.75$. Solid line: N 1s $\rightarrow \pi_1$*, $\beta = 24°$; dotted line: porphine C 1s $\rightarrow \pi$*, $\beta = 32°$; dashed line: phenyl C 1s $\rightarrow \pi$*, $\beta = 64°$.

as shown in Figure 4 (solid line), the polar angle β is estimated to be 24°. A similar polar angle of 28° was reported for ZnTPP on Ag/Cu substrates and interpreted as the average inclination angle between the molecular plane and the substrate.[46] However, recent studies of CoTPP monolayers on Cu(111) show that the complexes undergo saddle-shape distortion in the monolayer, such that two opposing pyrrole rings are tilted toward the surface by ∼20°, while the other two pyrrole rings point away from the surface by a similar angle.[36] This deformation, which was also observed by STM for tetraphenylporphyrin and various metallotetraphenylporphyrins,[14] can have a similar effect on the angular dependence of the NEXAFS spectra as an inclination of the undeformed molecule relative to the surface plane.[60] It cannot be excluded that the deformation of the molecules in the first layer also induces deformation of the following layers and that this contributes to the observed polar angle.

Using the same method, we also fitted the C K-edge NEXAFS spectra, assuming that the porphine macrocycle and phenyl substituents are independent π systems.[41,54] This fit results in a polar angle of 32° for the porphine system (see Figure 4, dotted line), which slightly deviates from the 24° obtained from the N K-edge NEXAFS spectra. Along the same lines of argument as used above, this polar angle can be interpreted as an overall inclination of the molecules relative to the substrate surface plane, but we again cannot exclude contributions from intramolecular deformation. Saddle-shape deformation (as was previously observed)[36] in combination with inclination would indeed explain why the C K-edge spectra show a larger polar angle than the N K-edge spectra: since mainly the C atoms at the periphery of the porphine ring are bent upward and downward, the C K-edge spectra should be more affected. Possibly, the overall inclination of the molecule relative to the surface is 24°, as derived from the N-edge resonances, whereas the pyrrole groups are tilted by additional ±8° relative to the original porphine plane, resulting in a value of 32° obtained from the C K-edge resonances.

By fitting the phenyl-related resonance in the C K-edge spectra, we obtain a polar angle of 64° relative to the surface plane (Figure 4, dashed line), which shows that the meso-phenyl rings are rotated out of the porphine plane. The origin of this

nonzero dihedral angle is well-understood and is related to the steric repulsion between the hydrogen atoms of the phenyl rings and the adjacent pyrrole moieties. The intramolecular repulsion energy rises steeply when the dihedral angle falls below 50° and exceeds 200 kJ/mol at 10°.[61] We note that the energy varies very little in the range between 60° and 90° (for example, by only 3.7 kJ/mol for CoTPP);[61] the angle can thus easily be influenced by intermolecular interactions. It is therefore not surprising that the dihedral angles vary widely within this range; for example, values of 80° for solid CoTPP[62] and 89° for solid FeTPP(OH)(H_2O)[63] have been reported. Upon adsorption on a surface, a delicate balance between maximization of the molecule−surface interaction and minimization of the intramolecular repulsion is established, such that the total adsorption energy is maximized.[14,30,61,63−68]

A precise determination of the dihedral angle in our case is hampered by the overall inclination of the molecules relative to the surface, which affects the orientation of the four peripheral phenyl rings relative to the surface differently. Only if we consider the extreme (and unlikely) case that the observed polar angle of 24° for the porphine system is entirely due to intramolecular deformation, i.e., that the (deformed) molecules lie parallel to the surface, the dihedral angle can be easily determined; it is then identical to the polar angle, 64°. Despite the critical assumption on which it is based, this value is in good agreement with the dihedral angles for solid 2HTPP (61.0° and 63.1°)[65] and for tetrapyridylporphyrin monolayers on Ag(111) (60°).[33,37] Similar values have been calculated for the gas-phase structures of ZnTPP and CoTPP (67°)[61] as well as for tetramesitylporphyrin (61°).[29]

However, the C and N K-edge resonances strongly suggest that the molecule is inclined relative to the surface, which makes an unambiguous determination of the dihedral angle impossible. To illustrate the difficulties, we assume that the axis, around which the porphine plane is rotated out of parallelity to the surface, passes through two of the phenyl rings. For these two rings, the inclination angle of the porphine (24°) then either adds to the measured polar angle or must be subtracted. In the first case we arrive at 88° and in the second at 40° for the dihedral angle. While the larger of the values falls in the range of minimum intramolecular repulsion (60°−90°), the value of 40° would lead to intramolecular strain and result in an energy increase of up to 54.8 kJ/mol (value for ZnTPP)[61] and is therefore less likely. We emphasize that this consideration ignores the contribution of the other two phenyl rings, whose dihedral angle is differently, but less affected by the inclination of the porphine ring. Furthermore, the porphine rings may be rotated around any other axis (or more likely a range of different axes) such that the angular dependence of the intensities is determined by a complex ensemble average.

3.2. Monolayer Preparation and Thermal Stability. Following the procedure of our previous work for the preparation 2HTPP monolayers on Ag(111),[24] we first evaporate a thin film of 2HTPP (∼7 monolayers) onto Au(111) at room temperature and then gradually increase the substrate temperatures in order to desorb excessive porphyrin molecules. During this process, temperature-dependent XPS measurements in the C 1s region were performed. The results are displayed in Figure 5.

Through analysis of the C 1s XPS data, information about the thermal stability of the adsorbed porphyrins, in particular with respect to the temperature window between multilayer desorption and monolayer decomposition, is obtained. In agreement with previous studies of 2HTPP and CoTPP on Ag(111),[24] only one combined signal at 285.0 eV is detected in

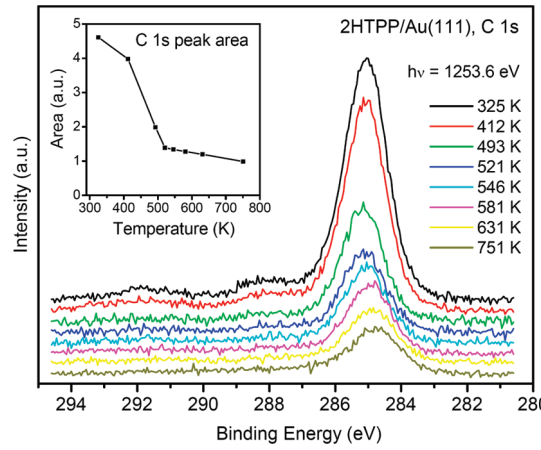

Figure 5. C 1s XP spectra of 2HTPP/Au(111) with an initial coverage of ∼7 monolayers at 300 K and subsequent heating to the following temperatures: 325, 412, 493, 521, 546, 581, 631, and 751 K. All spectra were taken at 300 K. The pass energy was set to be 20 eV. The inset shows the integrated area of the C 1s signals as a function of temperature.

the C 1s spectra due to the similar binding energies for the aromatic carbon atoms. In the 2HTPP multilayer spectrum (300 K), the two shakeup satellites at 291.8 and 288.1 eV are typical for organic molecules with aromatic π-conjugated systems.[69] With increasing substrate temperature, the main signal at 285 eV loses intensity (especially between 412 and 521 K) and shifts slightly (by less than 0.3 eV) toward lower binding energy, indicating multilayer desorption in this temperature range. This shift correlates well with that observed for CoTPP on Ag(111)[24] and is most likely due to relaxation, since the metal surface can provide a more efficient screening of the final hole state than the molecules in the multilayer. Note that at and above 631 K an additional shift to lower binding energies is observed, accompanied by a broadening of the peak from 1.4 to 1.6 eV full width at half-maximum (fwhm). This is ascribed to the thermal decomposition of 2HTPP on Au(111), which starts apparently between 581 and 631 K. Thus, the 2HTPP molecules on Au(111) are stable up to at least 581 K, which implies that the temperature window between multilayer desorption and monolayer decomposition has a width of at least 60 K. Desorption of 2HTPP multilayers can therefore be used to prepare 2HTPP monolayers. The overall temperature-induced changes of 2HTPP on Au(111) are very similar to those of CoTPP monolayers on Ag(111).[24] In both cases, the molecules in the monolayer cannot be desorbed intact.

For comparison, monolayers of NiTPP on Au(111) were prepared using the same procedure as introduced above. A series of temperature-dependent C 1s XPS measurements were performed for monitoring desorption of a NiTPP multilayer (∼14 monolayers), which was prepared by vapor deposition at a sample temperature of 300 K. The results are shown in Figure 6. Similar to the above observation for 2HTPP on Au(111) and also previous studies of CoTPP on Ag(111),[24] it was found that a temperature of ∼520 K is sufficient for a complete desorption of the multilayers and the formation of a NiTPP monolayer. This monolayer is stable up to at least ∼570 K, after which it starts to decompose.

3.3. Metalation of 2HTPP Monolayers on Au(111). In this section, we describe the reaction between 2HTPP molecules in the monolayer and coadsorbed Ni atoms. First, a 2HTPP monolayer was produced through vapor deposition of a multilayer onto Au(111) at 300 K and subsequent heating to 550 K, as described in section 3.2. After this, small amounts of nickel

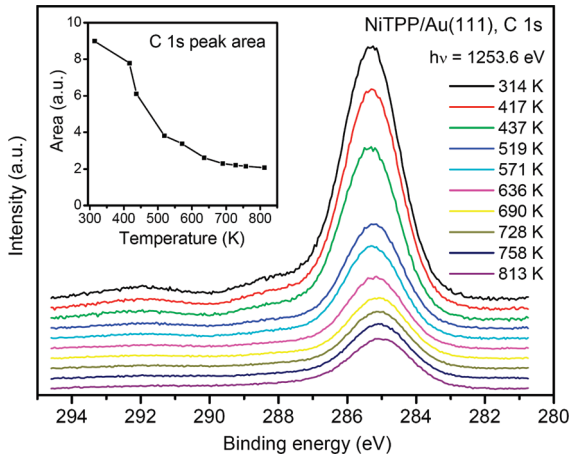

Figure 6. C 1s XP spectra of NiTPP/Au(111) with an initial coverage of 14 monolayers at 300 K and subsequent heating to the following temperatures: 314, 417, 437, 519, 571, 636, 690, 728, 758, and 813 K. All spectra were taken at 300 K. The pass energy was set to be 50 eV. The inset shows the integrated C 1s peak area as a function of temperature.

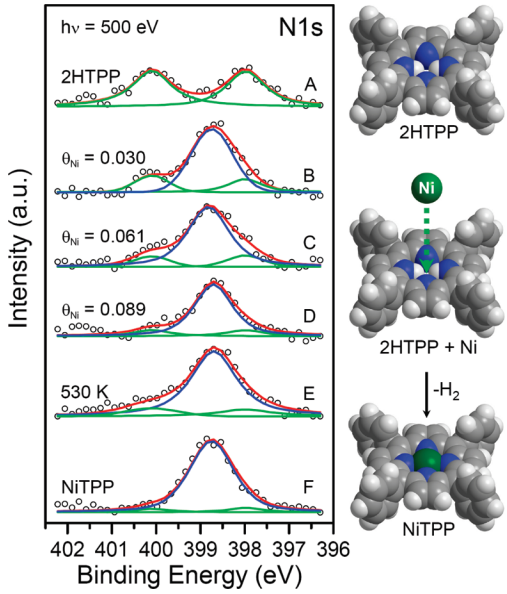

Figure 7. N 1s XP spectra of (A) a monolayer of 2HTPP on Au(111) and after incremental deposition of Ni up to (B) $\theta_{Ni} = 0.030$, (C) 0.061, and (D) 0.089 at 300 K, and (E) after heating sample D to 530 K. (F) N 1s photoemission spectrum of a NiTPP monolayer on Au(111) for comparison. The photon energy was 500 eV.

atoms were deposited in several successive steps. The reaction progress was monitored by means of N 1s XP spectra (Figure 7), which provide direct information regarding the chemical state of the coordinating nitrogen atoms of the porphine system. Here, we used monochromatized synchrotron radiation with a photon energy of $h\nu = 500$ eV for excitation, since it provides better surface sensitivity and higher energy resolution as compared to our nonmonochromatized laboratory X-ray source. Figure 7A shows the N 1s spectrum of a monolayer of 2HTPP on Au(111). It contains two well-separated components with binding energies of 400.1 and 398.0 eV, which are assigned to the two chemically different types of nitrogen atoms in 2HTPP, pyrrolic nitrogen (−NH−) and iminic nitrogen (=N−), respectively. The peak positions and relative intensities are in excellent agreement with previous studies.[15,16,19,27]

The deposition of a small amount of Ni, $\theta_{Ni} = 0.030$, onto the 2HTPP monolayer causes substantial changes in the N 1s signal (see Figure 7B): the original two separate N 1s components of 2HTPP lose intensity while a new component appears at 398.8 eV. By comparison with the N 1s signal of a monolayer of NiTPP which was *directly* deposited on Au(111) (Figure 7F), this new component is attributed to NiTPP formed by direct metalation of the 2HTPP molecules with the vapor-deposited Ni atoms. A similar N 1s component with almost the same position has been observed previously by direct metalation of 2HTPP on Ag(111) with Fe, Co, and Zn.[15,16,19,27] Further nickel deposition up to a total coverage of $\theta_{Ni} = 0.061$, which already exceeds the stoichiometric coverage of $\theta_{Ni} = 0.037$, leads to a slight increase of the new component at the expense of the two 2HTPP-related peaks (Figure 7C). If the Ni deposition is continued up to a total coverage of $\theta_{Ni} = 0.089$, the NiTPP-related N 1s signal becomes even more dominant, as shown in Figure 7D. Note that at this point all N 1s intensities are slightly smaller (by 24%) than before, most likely because the superabundant Ni atoms form clusters on the surface, which leads to increased signal damping. To investigate whether a higher degree of metalation can be achieved when increasing the sample temperature, we annealed the sample with $\theta_{Ni} = 0.089$ on the 2HTPP monolayer to 530 K and subsequently took the N 1s spectrum (Figure 7E) after cooling to room temperature. In fact, the intensity ratio between the metalation-induced N 1s component and the original two 2HTPP N 1s components remains almost unchanged, while the intensity of all N 1s components become larger (by 48%) than before. This indicates that no further metalation occurs, similar to the case of Fe/2HTPP on Ag(111).[19] The increased N 1s intensity may indicate that, upon heating, the excess Ni diffuses partly into the bulk or is covered by porphyrins; both would lead to reduced damping of the N 1s signal. The strong resemblance of the N 1s spectra of the in situ metalated porphyrin and the directly deposited NiTPP provides clear evidence that the Ni atom was successfully coordinated by the porphyrin, most likely following the equation

$$\mathrm{Ni(ads)} + \mathrm{2HTPP(ads)} \rightarrow \mathrm{NiTPP(ads)} + \mathrm{H_2(g)} \quad (2)$$

According to a previous study, the pyrrolic hydrogen atoms are transferred to the metal atom to form weakly bound H_2, which desorbs from the surface immediately.[15] Because of background subtraction problems, precise determination of the maximum degree of metalation is difficult. By comparing the integral of the NiTPP-related peak in Figure 7D,E with the total integral of the N 1s signal in each spectrum, we estimate that ∼81% of the porphyrins were metalated.

To obtain further evidence of NiTPP formation, we monitored the changes of the Ni $2p_{3/2}$ photoemission signal, as displayed in Figure 8. Spectra A−C were taken after deposition of the same incremental amounts of Ni onto the 2HTPP monolayer as in Figure 7B−D. Upon deposition of $\theta_{Ni} = 0.030$ at 300 K, two well-separated peaks emerge at 855.4 and 852.9 eV, respectively. As the Ni coverage increases, both peaks intensify disproportionally, with the one at 852.9 eV increasing more intensively. In order to clarify the different chemical states of Ni during the metalation, Ni $2p_{3/2}$ spectra of a NiTPP monolayer (Figure 8D) and metallic Ni ($\theta_{Ni} = 0.104$) directly deposited onto the Au(111) surface (Figure 8E) are also presented for comparison. Apparently, the position of the left peak at 855.4 eV in the spectra A−C is virtually identical to the Ni $2p_{3/2}$ peak position for a NiTPP monolayer. This provides further evidence that the Ni atoms are coordinated by 2HTPP to form NiTPP following reaction 2. The right peak at the low binding energy

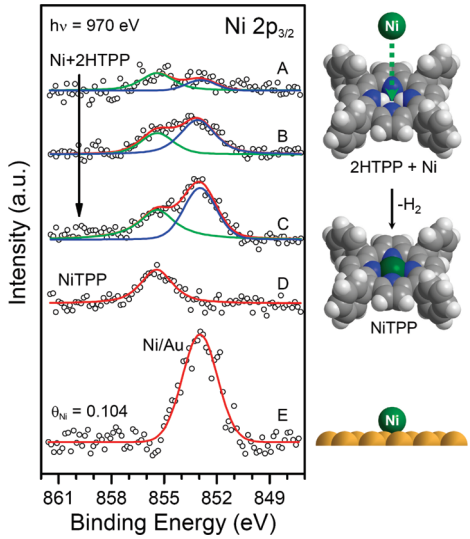

Figure 8. Ni $2p_{3/2}$ XP spectra of (A) $\theta_{Ni} = 0.030$, (B) 0.061, and (C) 0.089 Ni deposited on a monolayer of 2HTPP on Au(111); (D) a monolayer of NiTPP on Au(111) and (E) $\theta_{Ni} = 0.104$ Ni on Au(111) for comparison. All Ni deposition was performed at 300 K. The photon energy was set to 970 eV.

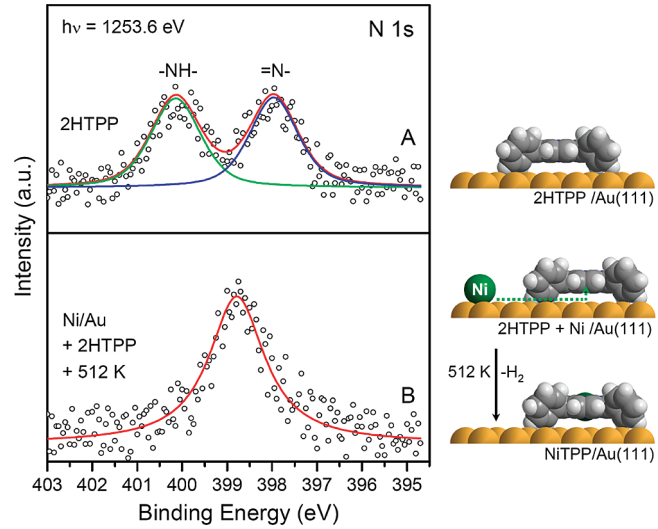

Figure 9. N 1s XP spectra of (A) a monolayer of 2HTPP on Au(111) and (B) Ni/Au(111) (with $\theta_{Ni} = 0.07$) followed by deposition of approximately two monolayers of 2HTPP and heating to 512 K. The red line in (B) is shown as a guide to the eyes.

side (852.9 eV) is located almost at the same position as that of metallic Ni directly deposited on Au(111). Since the intensity of this peak increases with deposition time, it can safely be assigned to unreacted metallic Ni, which is not coordinated by porphyrins. In conclusion, the results from the Ni $2p_{3/2}$ spectra agree excellently with those from the N 1s spectra; both provide unambiguous evidence for the formation of NiTPP by a surface-confined coordination reaction.

The fact that this metalation reaction proceeds rapidly and with high efficiency already at room temperature suggests that the activation barrier for NiTPP formation is very low. Similar findings have been reported for the reaction of Co and Fe with 2HTPP on Ag(111),[16,18,21] whereas metalation with Zn on Ag(111) has a substantial activation barrier of 130 kJ/mol.[27] Previous DFT calculations of the metalation mechanism by Shubina et al.[15] predict activation barriers for Ni in the range of 45−121 kJ/mol (depending on the functional used). A reaction that is fast at 300 K on the time scale of our experiment (several minutes) requires that its activation energy is below ~80 kJ/mol, if a frequency factor of the order of 10^{13} s^{-1} is assumed. Therefore, our experiment shows that the upper DFT value of 121 kJ/mol is certainly too high to be realistic.

3.4. Reaction of 2HTPP with Preadsorbed Ni on Au(111). Previous considerations concerning the mechanism of the surface-confined metalation reaction suggest that the metal atoms may first adsorb anywhere on the surface and then diffuse to the reaction sites of the porphyrins to undergo coordination.[14] At least, this must be the case if the metalation is performed with predeposited metal atoms, as was demonstrated for metalation of 2HTPP on Ag(111) with predeposited Fe or Zn.[19,27] Here, we followed a similar procedure to investigate the metalation with Ni on Au(111); i.e., Ni was deposited first using nearly twice the stoichiometric amount ($\theta_{Ni} = 0.07$), followed by approximately two monolayers of 2HTPP. Subsequently, the sample was heated to 512 K to induce the reaction. (Reaction at room temperature was not observed on the time scale of our XPS experiment.)

Evidence for the metalation is again obtained by the disappearance of the two 2HTPP-related N 1s signals combined with the appearance of a new peak at 398.8 eV (Figure 9). Comparison to

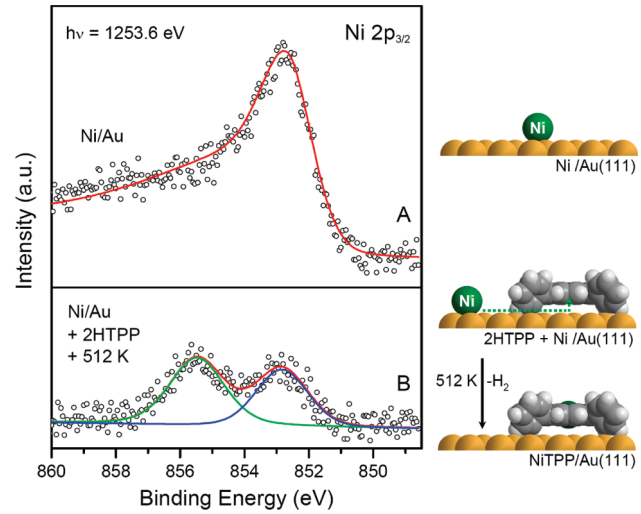

Figure 10. Ni $2p_{3/2}$ XP spectra of (A) Ni on Au(111) ($\theta_{Ni} = 0.07$) and (B) after deposition of approximately two monolayers of 2HTPP at 300 K on the Ni/Au(111) surface and subsequent heating to 512 K. The red line in (A) is shown as a guide to the eyes.

Figure 7F shows that this single new peak is clearly related to the NiTPP complex, indicating that 2HTPP has successfully "picked up" the Ni atoms from the Au(111) surface and coordinated them. It is the first time that such a reaction has been observed for Ni, and it is also the first porphyrin metalation with predeposited metal observed on an Au surface.

Additional evidence for the metalation reaction is provided by Figure 10, which displays the related Ni $2p_{3/2}$ spectra. When Ni ($\theta_{Ni} = 0.07$) was deposited onto the Au(111) surface, only one peak at 852.9 eV occurs in the Ni $2p_{3/2}$ XP spectrum. This peak is attributed to metallic Ni (Figure 10A). After depositing 2HTPP on the Ni/Au(111) substrate and heating to 512 K, a new peak at 855.4 eV has developed at the expense of the peak at 852.9 eV for metallic Ni. According to the analysis in section 3.3, this new peak can clearly be assigned to coordinated Ni ions in the NiTPP complex. This again confirms the formation of NiTPP. Because we deposited nearly twice the stoichiometric amount of Ni needed for the metalation of a monolayer of 2HTPP, it is expected that still some metallic Ni remains on the surface. Indeed, the metallic Ni $2p_{3/2}$ signal is still observable after annealing. This observation

also shows that only molecules in the first 2HTPP monolayer react with Ni, while excessive 2HTPP in the second layer (note that two monolayers of 2HTPP were deposited) desorbs during the heating step before it is metalated.

Note that, different from the case of 2HTPP/Zn/Ag(111), where the excess of Zn atoms almost completely vanished from the surface after heating to 550 K,[19,27] the clear Ni $2p_{3/2}$ signal of metallic Ni is still detected, indicating that diffusion of Ni into the deep bulk of the Au crystal does obviously not occur after heating the surface to 512 K.

The reaction of 2HTPP molecules with preadsorbed Ni atoms requires that either the Ni atoms or the porphyrin molecules are sufficiently mobile on the surface to diffuse over distances of several nanometers on the time scale of our experiment. Diffusion of the 2HTPP molecules in a closed monolayer seems unlikely because the molecules would have to occupy temporarily sites in the second layer. If this would be possible, the molecules should also desorb intact because in both cases the direct bond between molecules and metal surface is completely broken. However, thermal desorption of intact molecules from the monolayer does not occur, and therefore we can exclude diffusion of the 2HTPP molecules within a complete monolayer. Hence, the metal atoms must be the mobile species. Surface diffusion of metal atoms has been studied quantitatively by perturbed angular correlation (PAC) spectroscopy for ^{111}In probes on Ag, Cu, and Pd surfaces.[70−72] Typical activation energies on coinage metals range from 0.31 eV (for adatom diffusion on Ag(100)) to 0.69 eV (for vacancy diffusion in a terrace) on Ag(111).[70] If we assume that Ni on Au(111) has similar diffusion activation energies, we can estimate the number of site change events per second. Using the above-noted values of 0.31 and 0.69 eV and assuming a frequency factor for diffusion in the order of 10^{12} s^{-1},[70] we estimate numbers of 6×10^6 and 2.5 events per second at 300 K, respectively. Thus, even the higher activation energy value (0.69 eV) for vacancy diffusion on a terrace is sufficiently low to allow for metal atom diffusion at room temperature. In our case, adatom diffusion may actually have a larger activation energy because the terraces are covered with a closed layer of porphyrins. Therefore, the vacancy diffusion mechanism may compete successfully because here the metal atoms migrate within the first layer of the Au substrate, i.e., beneath the organic layer. The fact that metalation with preadsorbed Ni requires heating to >500 K is probably related to the formation of Ni islands, which have a low two-dimensional vapor pressure at room temperature. It is therefore likely that the removal of Ni atoms from the islands is the rate-limiting step. This assumption is supported by previous studies of porphyrin metalation with Fe on Ag(111), where formation of islands at the step edges and their dissolution in the presence of a porphyrin layer and at elevated temperatures was directly observed with STM.[19]

3.5. Electronic Interaction of NiTPP with a Au(111) Surface. The Ni $2p_{3/2}$ spectra in Figures 8 and 10 also give insight into the character of the electronic interaction between the coordinated Ni ions and the Au(111) substrate. The data show that the Ni $2p_{3/2}$ BE of metallic Ni (submonolayer) is lower than the BE of a NiTPP monolayer; the BE difference is 2.5 eV. This chemical shift reflects the different oxidation states (Ni^0 vs Ni^{2+}) of the two Ni species and indicates that the Ni^{2+} ions in NiTPP monolayer retain their nominal oxidation state in the presence of the substrate, which is not always the case when planar metal complexes bind to metal surfaces. For CoTPP monolayers on Ag(111), the Co $2p_{3/2}$ BE is by 1.8 eV lower than the respective BE for the CoTPP multilayer and is almost identical to the BE of metallic Co^0 on Ag(111). This finding has been ascribed to transfer of electron density from the Ag substrate to the Co ion, in conjunction with the formation of a covalent (or metallic) bond between metal center and substrate.[22,24] Similar observations have been made for iron(II) tetraphenylporphyrin (FeTPP) and iron(II) phthalocyanine (FePc) on Ag(111).[19,20] For cobalt(II) tetraphenylporphyrin (CoTPP) and octaethylporphyrin (CoOEP) on Au(111), however, it was found that only a fraction of the complexes interact strongly with the substrate, resulting in a BE shift of 1.6 eV (CoOEP) and 2.0 eV (CoTPP) between multilayer and monolayer, whereas the majority of the complexes is much less influenced by the substrate. This nonuniform behavior has been attributed to the herringbone reconstruction of the Au(111) surface, which leads to lateral inhomogeneities in the reactivity of the Au surface.[26]

The fact that the Ni $2p_{3/2}$ signal of NiTPP monolayers on Au(111) shows no significant signal splitting and is well separated from the signal of Ni^0 indicates that its interaction with the Au substrate is even weaker than that of CoTPP. Most likely, this is due to the lower energy of the Ni 3d levels as compared to the Co 3d and Fe 3d levels.

4. Conclusion

2HTPP multilayers on Au(111), obtained by vapor deposition at a sample temperature of 300 K, are well ordered and show preferential orientation of the molecules. The experimental polar angle of ∼24°−32° can be interpreted as the average inclination angle between porphyrin plane and substrate, but adsorption-induced deformation of the molecules may also contribute to a nonzero polar angle. As expected, the phenyl substituents are rotated out of the porphyrin plane. Monolayers of 2HTPP and NiTPP on Au(111) can be prepared by vapor deposition of multilayers onto the Au(111) surface and subsequent thermal desorption of the excessive layers. The monolayers of both molecules are thermally stable up to at least 580 K. NiTPP can be synthesized in situ via direct metalation of 2HTPP monolayers with vapor-deposited Ni atoms. The reaction proceeds rapidly at room temperature with a high yield. Moreover, NiTPP is also formed by reaction of 2HTPP molecules with predeposited nickel atoms on Au(111); this reaction requires elevated temperatures. Additional evidence for the formation of NiTPP by surface-confined coordination reaction between 2HTPP and Ni is provided by comparison with XP spectra of directly deposited NiTPP. On the basis of Ni 2p XP spectra, it is concluded that the electronic interaction between the coordinated Ni ions and the gold surface is weak and does not lead to significant transfer of electron density from the substrate to the Ni ions.

Acknowledgment. J.F.Z. thanks the National Nature Surface Foundation of China through Grant No. 20773111, the Program for New Century Excellent Talents in University (NCET), and the "Hundred Talents Program" of the Chinese Academy of Sciences for financial support. J.M.G. thanks the Alexander von Humboldt Foundation for support through the Feodor-Lynen Alumni Program. We thank Rainer Fink and Hans-Peter Steinrück for discussions.

References and Notes

(1) Voet, D.; Voet, J. G. *Biochemistry*, 3rd ed.; John Wiley & Sons, Inc.: New York, 2004.

(2) Drain, C. M.; Varotto, A.; Radivojevic, I. *Chem. Rev.* **2009**, *109*, 1630–1658.

(3) Beletskaya, I.; Tyurin, V. S.; Tsivadze, A. Y.; Guilard, R.; Stern, C. *Chem. Rev.* **2009**, *109*, 1659–1713.

(4) Oliver, I. T.; Rawlinson, W. A. *Biochem. J.* **1955**, *61*, 641–646.

(5) Campbell, W. M.; Jolley, K. W.; Wagner, P.; Wagner, K.; Walsh, P. J.; Gordon, K. C.; Schmidt-Mende, L.; Nazeeruddin, M. K.; Wang, Q.; Gratzel, M.; Officer, D. L. *J. Phys. Chem. C* **2007**, *111*, 11760–11762.

(6) Paolesse, R.; Di Natale, C.; Dall'Orto, V. C.; Macagnano, A.; Angelaccio, A.; Motta, N.; Sgarlata, A.; Hurst, J.; Rezzano, I.; Mascini, M.; D'Amico, A. *Thin Solid Films* **1999**, *354*, 245–250.

(7) Maree, C. H. M.; Roosendaal, S. J.; Savenije, T. J.; Schropp, R. E. I.; Schaafsma, T. J.; Habraken, F. *J. Appl. Phys.* **1996**, *80*, 3381–3389.

(8) Harima, Y.; Okazaki, H.; Kunugi, Y.; Yamashita, K.; Ishii, H.; Seki, K. *Appl. Phys. Lett.* **1996**, *69*, 1059–1061.

(9) Palacin, S.; Ruaudel-Teixier, A.; Barraud, A. *J. Phys. Chem.* **1989**, *93*, 7195–7199.

(10) Watcharinyanon, S.; Puglia, C.; Gothelid, E.; Backvall, J. E.; Moons, E.; Johansson, L. S. O. *Surf. Sci.* **2009**, *603*, 1026–1033.

(11) Thomas, P. J.; Berovic, N.; Laitenberger, P.; Palmer, R. E.; Bampos, N.; Sanders, J. K. M. *Chem. Phys. Lett.* **1998**, *294*, 229–232.

(12) Berner, S.; Lidbaum, H.; Ledung, G.; Ahlund, J.; Nilson, K.; Schiessling, J.; Gelius, U.; Backvall, J. E.; Puglia, C.; Oscarsson, S. *Appl. Surf. Sci.* **2007**, *253*, 7540–7548.

(13) Hai, N. T. M.; Gasparovic, B.; Wandelt, K.; Broekmann, P. *Surf. Sci.* **2007**, *601*, 2597–2602.

(14) Gottfried, J. M.; Marbach, H. *Z. Phys. Chem. (Muenchen, Ger.)* **2009**, *223*, 53–74.

(15) Shubina, T. E.; Marbach, H.; Flechtner, K.; Kretschmann, A.; Jux, N.; Buchner, F.; Steinrück, H. P.; Clark, T.; Gottfried, J. M. *J. Am. Chem. Soc.* **2007**, *129*, 9476–9483.

(16) Gottfried, J. M.; Flechtner, K.; Kretschmann, A.; Lukasczyk, T.; Steinrück, H. P. *J. Am. Chem. Soc.* **2006**, *128*, 5644–5645.

(17) Flechtner, K.; Kretschmann, A.; Bradshaw, L. R.; Walz, M. M.; Steinrück, H. P.; Gottfried, J. M. *J. Phys. Chem. C* **2007**, *111*, 5821–5824.

(18) Buchner, F.; Schwald, V.; Comanici, K.; Steinrück, H. P.; Marbach, H. *ChemPhysChem* **2007**, *8*, 241–243.

(19) Buchner, F.; Flechtner, K.; Bai, Y.; Zillner, E.; Kellner, I.; Steinrück, H. P.; Marbach, H.; Gottfried, J. M. *J. Phys. Chem. C* **2008**, *112*, 15458–15465.

(20) Bai, Y.; Buchner, F.; Wendahl, M. T.; Kellner, I.; Bayer, A.; Steinrück, H. P.; Marbach, H.; Gottfried, J. M. *J. Phys. Chem. C* **2008**, *112*, 6087–6092.

(21) Auwärter, W.; Weber-Bargioni, A.; Brink, S.; Riemann, A.; Schiffrin, A.; Ruben, M.; Barth, J. V. *ChemPhysChem* **2007**, *8*, 250–254.

(22) Flechtner, K.; Kretschmann, A.; Steinrück, H. P.; Gottfried, J. M. *J. Am. Chem. Soc.* **2007**, *129*, 12110–12111.

(23) Barlow, D. E.; Scudiero, L.; Hipps, K. W. *Langmuir* **2004**, *20*, 4413–4421.

(24) Lukasczyk, T.; Flechtner, K.; Merte, L. R.; Jux, N.; Maier, F.; Gottfried, J. M.; Steinrück, H. P. *J. Phys. Chem. C* **2007**, *111*, 3090–3098.

(25) Bai, Y.; Buchner, F.; Kellner, I.; Schmid, M.; Vollnhals, F.; Steinrück, H. P.; Marbach, H.; Gottfried, J. M. *New J. Phys.* **2009**, *11*, 125004.

(26) Bai, Y.; Sekita, M.; Schmid, M.; Bischof, T.; Steinrück, H.-P.; Gottfried, J. M. *Phys. Chem. Chem. Phys.* **2010**, *12*, 4336−4344.

(27) Kretschmann, A.; Walz, M. M.; Flechtner, K.; Steinrück, H. P.; Gottfried, J. M. *Chem. Commun.* **2007**, 568–570.

(28) Weber-Bargioni, A.; Reichert, J.; Seitsonen, A. P.; Auwärter, W.; Schiffrin, A.; Barth, J. V. *J. Phys. Chem. C* **2008**, *112*, 3453–3455.

(29) Ecija, D.; Trelka, M.; Urban, C.; de Mendoza, P.; Mateo-Marti, E.; Rogero, C.; Martin-Gago, J. A.; Echavarren, A. M.; Otero, R.; Gallego, J. M.; Mirandat, R. *J. Phys. Chem. C* **2008**, *112*, 8988–8994.

(30) Buchner, F.; Comanici, K.; Jux, N.; Steinrück, H. P.; Marbach, H. *J. Phys. Chem. C* **2007**, *111*, 13531–13538.

(31) Scudiero, L.; Barlow, D. E.; Mazur, U.; Hipps, K. W. *J. Am. Chem. Soc.* **2001**, *123*, 4073–4080.

(32) Scudiero, L.; Barlow, D. E.; Hipps, K. W. *J. Phys. Chem. B* **2002**, *106*, 996–1003.

(33) Scudiero, L.; Barlow, D. E.; Hipps, K. W. *J. Phys. Chem. B* **2000**, *104*, 11899–11905.

(34) Hipps, K. W.; Barlow, D. E.; Mazur, U. *J. Phys. Chem. B* **2000**, *104*, 2444–2447.

(35) Krasnikov, S. A.; Beggan, J. P.; Sergeeva, N. N.; Senge, M. O.; Cafolla, A. A. *Nanotechnology* **2009**, *20*, 135301. .

(36) Weber-Bargioni, A.; Auwärter, W.; Klappenberger, F.; Reichert, J.; Lefrancois, S.; Strunskus, T.; Wöll, C.; Schiffrin, A.; Pennec, Y.; Barth, J. V. *ChemPhysChem* **2008**, *9*, 89–94.

(37) Auwärter, W.; Weber-Bargioni, A.; Riemann, A.; Schiffrin, A.; Groning, O.; Fasel, R.; Barth, J. V. *J. Chem. Phys.* **2006**, *124*, 194708.

(38) Katsonis, N.; Vicario, J.; Kudernac, T.; Visser, J.; Pollard, M. M.; Feringa, B. L. *J. Am. Chem. Soc.* **2006**, *128*, 15537–15541.

(39) Polzonetti, G.; Carravetta, V.; Iucci, G.; Ferri, A.; Paolucci, G.; Goldoni, A.; Parent, P.; Laffon, C.; Russo, M. V. *Chem. Phys.* **2004**, *296*, 87–100.

(40) Krasnikov, S. A.; Sergeeva, N. N.; Brzhezinskaya, M. M.; Preobrajenski, A. B.; Sergeeva, Y. N.; Vinogradov, N. A.; Cafolla, A. A.; Senge, M. O.; Vinogradov, A. S. *J. Phys.: Condens. Matter* **2008**, *20*, 235207. 6pp.

(41) Goldoni, A.; Cudia, C. C.; Vilmercati, P.; Larciprete, R.; Cepek, C.; Zampieri, G.; Sangaletti, L.; Pagliara, S.; Verdini, A.; Cossaro, A.; Floreano, L.; Morgante, A.; Petaccia, L.; Lizzit, S.; Battocchio, C.; Polzonetti, G. *Surf. Sci.* **2006**, *600*, 4013–4017.

(42) Ferri, A.; Polzonetti, G.; Iucci, G.; Paolucci, G.; Goldoni, A.; Parent, P.; Laffon, C.; Contini, G.; Carravetta, V. *Surf. Interface Anal.* **2000**, *30*, 407–409.

(43) Wende, H.; Bernien, M.; Luo, J.; Sorg, C.; Ponpandian, N.; Kurde, J.; Miguel, J.; Piantek, M.; Xu, X.; Eckhold, P.; Kuch, W.; Baberschke, K.; Panchmatia, P. M.; Sanyal, B.; Oppeneer, P. M.; Eriksson, O. *Nat. Mater.* **2007**, *6*, 516–520.

(44) Bernien, M.; Xu, X.; Miguel, J.; Piantek, M.; Eckhold, P.; Luo, J.; Kurde, J.; Kuch, W.; Baberschke, K.; Wende, H.; Srivastava, P. *Phys. Rev. B* **2007**, *76*, 214406.

(45) Cudia, C. C.; Vilmercati, P.; Larciprete, R.; Cepek, C.; Zampieri, G.; Sangaletti, L.; Pagliara, S.; Verdini, A.; Cossaro, A.; Floreano, L.; Morgante, A.; Petaccia, L.; Lizzit, S.; Battocchio, C.; Polzonetti, G.; Goldoni, A. *Surf. Sci.* **2006**, *600*, 4013–4017.

(46) Narioka, S.; Ishii, H.; Ouchi, Y.; Yokoyama, T.; Ohta, T.; Seki, K. *J. Phys. Chem.* **1995**, *99*, 1332–1337.

(47) Checcoli, P.; Conte, G.; Salvatori, S.; Paolesse, R.; Bolognesi, A.; Berliocchi, A.; Brunetti, F.; D'Amico, A.; Di Carlo, A.; Lugli, P. *Synth. Met.* **2003**, *138*, 261–266.

(48) Che, C. M.; Xiang, H. F.; Chui, S. S. Y.; Xu, Z. X.; Roy, V. A. L.; Yan, J. J.; Fu, W. F.; Lai, P. T.; Williams, I. D. *Chem. Asian J.* **2008**, *3*, 1092–1103.

(49) Tian, X. Y.; Xu, Z.; Zhang, F. J.; Zhao, S. L.; Yuan, G. C.; Li, J.; Sun, Q. J.; Wang, Y. *Curr. Appl. Phys.* **2010**, *10*, 129–132.

(50) Karl, N. *Synth. Met.* **2003**, *133*, 649–657.

(51) Stöhr, J. *NEXAFS Spectroscopy*; Springer Series in Surface Sciences; Springer-Verlag: Berlin, 1992; Vol. 25.

(52) Sakai, T.; Ishikawa, K.; Takezoe, H.; Matsuie, N.; Yamamoto, Y.; Ishii, H.; Ouchi, Y.; Oji, H.; Seki, K. *J. Phys. Chem. B* **2001**, *105*, 9191–9195.

(53) http://www.webelements.com/.

(54) de Jong, M. P.; Friedlein, R.; Sorensen, S. L.; Öhrwall, G.; Osikowicz, W.; Tengsted, C.; Jönsson, S. K. M.; Fahlman, M.; Salaneck, W. R. *Phys. Rev. B* **2005**, *72*, 035448.

(55) Sham, T. K.; Yang, B. X.; Kirz, J.; Tse, J. S. *Phys. Rev. A* **1989**, *40*, 652–669.

(56) Francis, J. T.; Hitchcock, A. P. *J. Phys. Chem.* **1992**, *96*, 6598–6610.

(57) Nilsson, D.; Watcharinyanon, S.; Eng, M.; Li, L. Q.; Moons, E.; Johansson, L. S. O.; Zharnikov, M.; Shaporenko, A.; Albinsson, B.; Martensson, J. *Langmuir* **2007**, *23*, 6170–6181.

(58) Polzonetti, G.; Ferri, A.; Russo, M. V.; Iucci, G.; Licoccia, S.; Paolesse, R. *J. Vac. Sci. Technol. A* **1999**, *17*, 832–839.

(59) Newbury, D. C.; Ishii, I.; Hitchcock, A. P. *Can. J. Chem.* **1986**, *64*, 1145–1155.

(60) Mainka, C.; Bagus, P. S.; Schertel, A.; Strunskus, T.; Grunze, M.; Wöll, C. *Surf. Sci.* **1995**, *341*, L1055–L1060.

(61) Wölfle, T.; Görling, A.; Hieringer, W. *Phys. Chem. Chem. Phys.* **2008**, *10*, 5739–5742.

(62) Madura, P.; Scheidt, W. R. *Inorg. Chem.* **1976**, *15*, 3182–3184.

(63) Fleischer, E. B.; Miller, C. K.; Webb, L. E. *J. Am. Chem. Soc.* **1964**, *86*, 2342.

(64) Stevens, E. D. *J. Am. Chem. Soc.* **1981**, *103*, 5087–5095.

(65) Silvers, S. J.; Tulinsky, A. *J. Am. Chem. Soc.* **1967**, *89*, 3331–3337.

(66) Pan, L.; Kelly, S.; Huang, X. Y.; Li, J. *Chem. Commun.* **2002**, 2334–2335.

(67) Moresco, F.; Meyer, G.; Rieder, K. H.; Ping, H.; Tang, H.; Joachim, C. *Surf. Sci.* **2002**, *499*, 94–102.

(68) Jung, T. A.; Schlittler, R. R.; Gimzewski, J. K. *Nature* **1997**, *386*, 696–698.

(69) Schöll, A.; Zou, Y.; Jung, M.; Schmidt, T.; Fink, R.; Umbach, E. *J. Chem. Phys.* **2004**, *121*, 10260–10267.

(70) Fink, R.; Wesche, R.; Klas, T.; Krausch, G.; Platzer, R.; Voigt, J.; Wöhrmann, U.; Schatz, G. *Surf. Sci.* **1990**, *225*, 331–340.

(71) Klas, T.; Fink, R.; Krausch, G.; Platzer, R.; Voigt, J.; Wesche, R.; Schatz, G. *Europhys. Lett.* **1988**, *7*, 151–157.

(72) Fink, R.; Runge, B. U.; Jacobs, K.; Krausch, G.; Lohmüller, J.; Luckscheiter, B.; Wöhrmann, U.; Schatz, G. *J. Phys.: Condens. Matter* **1993**, *5*, 3837–3842.

JP102031M